

Effects of Laser Wavelength on Hot Electrons Produced by Ultrashort Intense Laser Pulse on Solid-Density Targets

KATO Susumu¹⁾, MIURA Eisuke¹⁾, TAKAHASHI Eiichi¹⁾, NAKAMURA Tatsufumi²⁾,
KATO Tomokazu²⁾ and OWADANO Yoshiro¹⁾

¹⁾National Institute of Advanced Industrial Science and Technology (AIST), Tsukuba, Ibaraki 305-8568, Japan

²⁾Department of Applied Physics, Waseda University, Tokyo 169-8555, Japan

(Received 26 June 2002 / Accepted 3 July 2002)

The hot electron temperature and electron energy spectrum of intense laser plasma interactions are reexamined from a viewpoint of the difference in laser wavelength. The hot electron temperature measured by a particle-in-cell simulation is scaled by $I\lambda^{-1}$ rather than $I\lambda^2$ at the interaction with overdense plasmas, where I and λ are the laser intensity and wavelength, respectively.

Keywords: ultraintense laser, hot electron production, laser-plasma interactions, solid-density plasma

High energy electron production by an intense ultrashort laser pulse has attracted much interest as a possible fast ignitor in inertial fusion energy [1]. Ultraintense irradiation experiments using an infrared subpicosecond laser, e.g., Nd:glass ($\lambda = 1,053$ nm) or Ti:sapphire ($\lambda = 800$ nm) lasers, whose powers and focused intensities exceed 100 TW and 10^{20} W/cm², are possible using chirped pulse amplification techniques [2]. In these experiments, the classical normalized momentum of electrons $a_0 \equiv P_{\text{osc}}/mc = (I\lambda_\mu^2/1.37 \times 10^{18})^{1/2} \geq 1$, where m is the electron mass, c is the speed of light, I is the laser intensity in W/cm², and λ_μ is the wavelength in μm . On the other hand, a KrF laser ($\lambda = 248$ nm) has an advantage as a fast ignitor in that the critical density is close to the core, and hot electron energies are suitable since the critical density of the KrF laser is ten times greater than that of an infrared laser [3]. However, the KrF laser irradiance intensities were only the order of 10^{18} W/cm², namely $a_0 < 1$ [4]. Therefore, the dependence of the laser plasma interactions on the laser wavelength is not investigated in $a_0 \geq 1$.

The absorption, electron energy spectrum, and hot electron temperature have usually been investigated and scaled using the parameters $I\lambda^2$, n_e/n_c , and L/λ [5,6], where n_e , n_c , and L are the electron density, critical density, and density scale length, respectively. Critical density absorption of the laser light converts laser energy into hot electrons having a suprathermal temperature T_h

approximately proportional to $\sqrt{I\lambda^2}$ for $a_0 > 1$, and $T_h \sim [(1 + a_0^2)^{1/2} - 1]mc^2$ at moderate density [7], where $mc^2 = 511$ keV is an electron rest mass. The scaling of the hot electron temperature has been supported by experiments of Nd:glass and Ti:sapphire lasers [8]. On the other hand, the results of one-dimensional simulation for normal incidence in the density region $4 < n_e/n_c < 100$ and the normalized intensity $4 < a_0^2 < 30$ have shown that $T_h \sim \eta(n_e/n_c)^\alpha [(1 + a_s^2)^{1/2} - 1]mc^2$, where $a_s = a_0(n_e/n_c)^{1/2}$ is the electromagnetic fields at the surface of the overdense plasma, $\eta = 0.5 \sim 1.1$ and $\alpha = 1/2$, which depend weakly on $I\lambda^2$ and n_e/n_c [6]. The hot electron temperature is scaled by the amplitude of electromagnetic fields at the plasma surface rather than that in the vacuum; namely, the hot electron temperature is slightly dependent on the wavelength.

In this Rapid Communications, the scaling of the hot electron temperature and the electron energy spectrum are reexamined from the viewpoint of the difference in laser wavelength by using a particle-in-cell (PIC) simulation code. Thus, the dependence of hot electron production — by ultrashort intense laser pulse on solid density plasmas — on the laser wavelength is clarified.

In order to investigate hot electron generation for oblique incidence, we use the relativistic 1 and 2/2 dimensional PIC simulation with the boost frame moving with $c \sin \theta$ parallel to the target surface, where c and θ are the speed of light and an angle of incidence [9]. In the simulation, the targets are the fully ionized plastic and

author's e-mail: s.kato@aist.go.jp

aluminum, and the electron densities are $n_{e0} \sim 3.5 \times 10^{23} \text{cm}^{-3}$ and $8.6 \times 10^{23} \text{cm}^{-3}$, respectively. The densities correspond to $n_{e0}/n_c = 20$ and 48 for $\lambda = 0.25 \mu\text{m}$, $n_{e0}/n_c = 78$ and 190 for $\lambda = 0.5 \mu\text{m}$, and $n_{e0}/n_c = 310$ and 770 for $\lambda = 1 \mu\text{m}$, respectively. The density profile has a sharp density gradient, $n_e(x) = n_{e0}$ for $x \geq 0$ and $n_e(x) = 0$ for $x < 0$. The laser pulse starts at $x < 0$ and propagates towards $x > 0$. The laser intensity rises in 5 fs and remains constant after that. The irradiated intensity $I = 5 \times 10^{19} \text{W/cm}^2$ and the angle of incidence $\theta = 30^\circ$ (p-polarized). $a_0^2 = 2.3, 9.2,$ and 36 for $\lambda = 0.25, 0.5,$ and $1 \mu\text{m}$, respectively. Normalized electron energy distributions after 50 fs are shown in Fig. 1(a) and 1(b) for the plastic and aluminum, respectively. The hot electron temperatures of the plastic are 190, 120, and 60 keV, for $\lambda = 0.25, 0.5,$ and $1 \mu\text{m}$, respectively. The hot electron temperatures of the aluminum are 170, 80, and 40 keV for $\lambda = 0.25, 0.5,$ and $1 \mu\text{m}$, respectively. Applying our simulation results of the hot electron temperature to $T_h \sim \eta(n_{e0}/n_c)^{1/2} [(1 + a_s^2)^{1/2} - 1] mc^2$, we obtained $\eta \sim 2.0$ and 2.8 for $\lambda = 0.25 \mu\text{m}$, $\eta \sim 0.63$ and 0.66 for $\lambda = 0.5 \mu\text{m}$, and $\eta \sim 0.16$ and 0.16 for $\lambda = 1 \mu\text{m}$, respectively. Namely, in the limit of $a_s \ll 1$, η is proportional to λ^{-2} . If the hot electron is generated by the ponderomotive potential of laser light at the surface, T_h is independent of the laser wavelength in the sharp density gradient [6]. In our simulation, however, $T_h \propto \lambda^{-1}$ instead of λ^0 or λ^1 . One of the reasons for this is the density profile modification by the laser. The density profile is strongly different between $\lambda = 0.25$ and $1 \mu\text{m}$ [11].

It is noted that T_h or η depends on the laser and plasma condition, e.g., the incident angle, polarization, and density scale length. For various laser and plasma conditions, more quantitative details of the energy and angular spectrum of the high energy electron will be investigated further in the future. The density profiles of both preformed plasma [12] and multi-dimensional effects such as surface deformation [7] are very important in these experiments.

A part of this study was financially supported by the Budget for Nuclear Research of the Ministry of Education, Culture, Sports, Science and Technology, based on the screening and counseling by the Atomic Energy Commission.

- [1] M. Tabak *et al.*, Phys. Plasmas **1**, 1626 (1994).
- [2] P. Maine *et al.*, IEEE J. Quantum Electron. **24**, 398 (1988); M.D. Perry *et al.*, Opt. Lett. **24**, 160 (1999).
- [3] M.J. Shaw *et al.*, Fusion Eng. Des. **44**, 209 (1999).
- [4] U. Teubner *et al.*, Phys. Rev. E **54**, 4167 (1996);

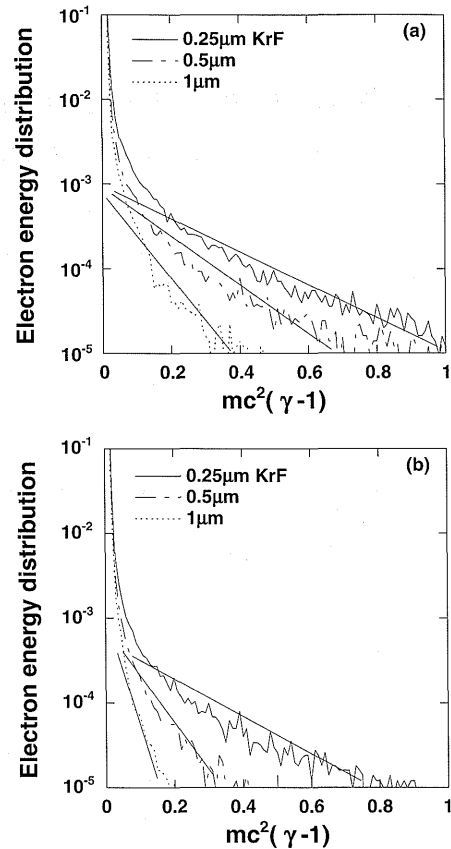


Fig. 1 Electron energy distribution at $t = 50$ fs and $I = 5 \times 10^{19} \text{W/cm}^2$ for (a) $n_{e0} = 3.5 \times 10^{23} \text{cm}^{-3}$ and (b) $n_{e0} = 8.6 \times 10^{23} \text{cm}^{-3}$, respectively. The solid, dashed-dotted, and dotted lines are for $\lambda = 0.25, 0.5,$ and $1 \mu\text{m}$, respectively.

- M. Borghesi *et al.*, Phys. Rev. E **60**, 7374 (1999).
- [5] E. Lefebvre and G. Bonnaud, Phys. Rev. E **55**, 1011 (1997).
- [6] S.C. Wilks and W.L. Kruer, IEEE J. Quantum Electron. **33**, 1954 (1997)
- [7] S.C. Wilks, Phys. Fluids **B 5**, 2603 (1993); S.C. Wilks *et al.*, Phys. Rev. Lett. **69**, 1383 (1992).
- [8] G. Malka and J.L. Miquel, Phys. Rev. Lett. **77**, 75 (1996); Y. Oishi *et al.*, Appl. Phys. Lett. **79**, 1234 (2001).
- [9] A. Bourdier, Phys. Fluids **26**, 1804 (1983); P. Gibbon and A.R. Bell, Phys. Rev. Lett. **68**, 1535 (1992).
- [10] W.L. Kruer and K.G. Estabrook, Phys. Fluids **28**, 430 (1985).
- [11] S. Kato *et al.*, Proc. of the International Symposium on Science of Super-Strong Field Interactions, Hayama, JAPAN, 2002.
- [12] Wei Yu *et al.*, Phys. Rev. Lett. **85**, 570 (2000); T.E. Cowan *et al.*, Phys. Rev. Lett. **84**, 903 (2000).